

Similar Structural Basis for Membrane Localization and Protein Priming by an RNA-dependent RNA Polymerase*

Received for publication, December 28, 2001, and in revised form, February 25, 2002
Published, JBC Papers in Press, February 27, 2002, DOI 10.1074/jbc.M112429200

John M. Lyle‡§, Amy Clewell‡¶, Kathryn Richmond‡, Oliver C. Richards||, Debra A. Hope**‡‡, Steve C. Schultz||§§, and Karla Kirkegaard‡¶¶

From the ‡Department of Microbiology and Immunology, Stanford University School of Medicine, Stanford, California 94305 and the Departments of ||Molecular, Cellular, and Developmental Biology and **Chemistry and Biochemistry, University of Colorado, Boulder, Colorado 80309

Protein primers are used to initiate genomic synthesis of several RNA and DNA viruses, although the structural details of the primer-polymerase interactions are not yet known. Poliovirus polymerase binds with high affinity to the membrane-bound viral protein 3AB but uridylylates only the smaller peptide 3B *in vitro*. Mutational analysis of the polymerase identified four surface residues on the three-dimensional structure of poliovirus polymerase whose wild-type identity is required for 3AB binding. These mutants also decreased 3B uridylylation, arguing that the binding sites for the membrane tether and the protein primer overlap. Mutation of flanking residues between the 3AB binding site and the polymerase active site specifically decreased 3B uridylylation, likely affecting steps subsequent to binding. The physical overlap of sites for protein priming and membrane association should facilitate replication initiation in the membrane-associated complex.

The replication of linear nucleic acids without loss of coding information from the ends is a problem that has been solved in several ways by cellular and viral genomes. Solutions include those used by vaccinia virus, which primes DNA replication from hairpins that can be refolded to regenerate the terminal sequences (1, 2), by *Drosophila*, which repair damaged chromosomal termini by recombination (3), by many eukaryotic cells, which add end-specific telomeric sequences postreplicatively, and by viruses such as adenovirus and $\Phi 29$, which use protein primers that are covalently linked to the initiating nucleotides (reviewed in Ref. 4). For mammalian positive-strand RNA viruses such as poliovirus and hepatitis C, two mechanisms are suspected: *de novo* initiation (5–8) and protein priming (9) from the genomic ends.

The protein primer for the synthesis of poliovirus RNA includes, at a minimum, the 22-amino acid viral peptide 3B (also called VPg), which is found covalently linked to the 5' ends of

all newly synthesized positive and negative strands. Poliovirus translates its proteins as a single, large polyprotein that is cleaved into the proteins required for virion formation, host modification, and RNA replication. In many cases, proteolytic precursors have functions distinct from those of the limit digestion products. Evidence for the use of 3B. As a protein primer comes from *in vitro* experiments in which it was demonstrated that 3B is uridylylated in the presence of UTP, the poliovirus RNA-dependent RNA polymerase (3D), and an RNA template (9). The RNA used to template the uridylylation of 3B can either be poly(A), poliovirus RNA, or the small cis replication enhancer RNA (10, 11), an internal sequence required for RNA replication in infected cells (12). Whether 3B itself serves as the primer within infected cells and how it is brought into the RNA replication complex are not yet known.

Evidence for direct binding between polymerase and 3B was observed in the two-hybrid system (13), although a stronger signal was observed between the polymerase and a larger polypeptide that contains the 3B, sequences, 3AB (13, 14). When mutations of 3AB were tested to identify those that disrupted interactions with the poliovirus polymerase in the two-hybrid system, only those that mapped within the 3B sequences were found to be disruptive (13). Therefore, it is likely that many of the direct contacts between the polymerase and 3AB are within the 3B sequence.

All positive-strand RNA viruses, from picornaviruses such as poliovirus and foot and mouth disease virus to flaviviruses such as Dengue and hepatitis C virus, form their RNA replication complexes in association with cytoplasmic membranes whose identity differs for different viruses (Refs. 15–17 and the references therein). Protein 3AB contains an extended hydrophobic domain and associates with membranes both *in vitro* and when expressed in isolation in tissue culture cells (18, 19). Membrane-bound 3AB has been recovered from *Escherichia coli* expression systems and found to both stimulate the proteolytic activity of the precursor of poliovirus polymerase, 3CD (20), and recruit soluble polymerase from solution (14). A specific interaction between 3AB and poliovirus polymerase can also be observed with purified, detergent-solubilized 3AB, which stimulates poliovirus polymerase activity (20–22) by stabilizing the polymerase complex with the template and primer (23, 24). These data have led to a model in which membrane-associated 3AB or one of its larger precursors (25) binds directly to the soluble RNA-dependent RNA polymerase, facilitating its recruitment to the membranes upon which viral RNA replication occurs.

Previously, it was shown that the V391L mutation in poliovirus polymerase confers a specific defect in the interaction of the polymerase with viral protein 3AB in the yeast two-hybrid system and *in vitro* (14). Val³⁹¹ is located near motif E, a motif

* This work was supported by National Institutes of Health Grant AI-42119. The costs of publication of this article were defrayed in part by the payment of page charges. This article must therefore be hereby marked "advertisement" in accordance with 18 U.S.C. Section 1734 solely to indicate this fact.

‡ A predoctoral fellow of the Howard Hughes Medical Institute.

¶ Present address: Bastyr University, 14500 Juanita Dr. NE, Kenmore, WA 98028.

‡‡ Present address: Cellomics Inc., 100 Technology Dr., Pittsburgh, PA 15219.

§§ Present address: Diné College, P. O. Box 251C, Tsaile, AZ 86556.

¶¶ To whom correspondence should be addressed: Dept. of Microbiology and Immunology, Stanford University School of Medicine, 299 Campus Dr., Stanford, CA 94305. Tel.: 650-498-7075; Fax: 650-498-7174; E-mail: karlak@stanford.edu.

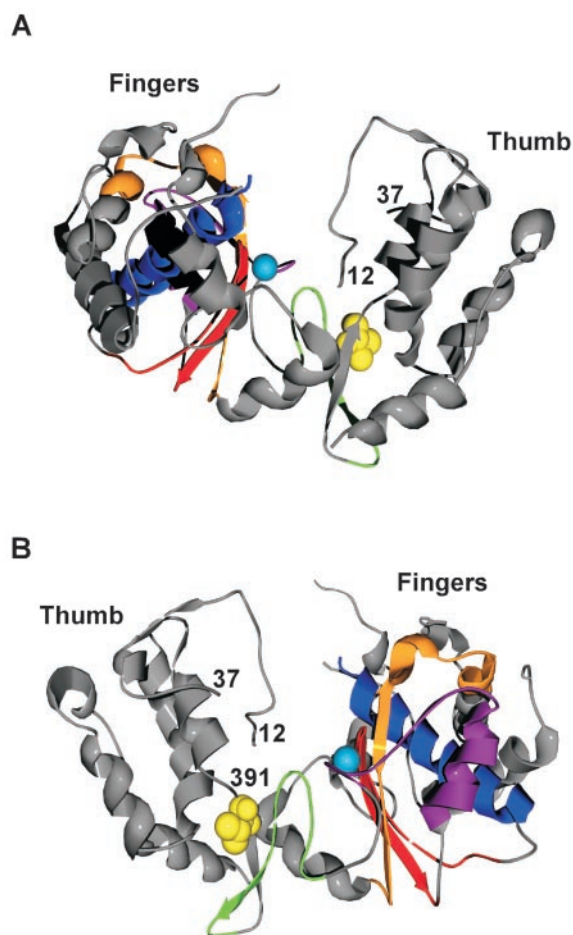


FIG. 1. **Ribbon diagram of the poliovirus RNA-dependent RNA polymerase, 3D.** The three-dimensional structure of poliovirus polymerase (26) resolves residues 12–37, 67–97, and 182–461. Residues 12–37 are thought to be donated intermolecularly (26, 30). Views from the front, facing the “palm” (A), and from the “back” of the polymerase “hand” (B) are shown. The five canonical RNA-dependent RNA polymerase domains are colored as follows: motif A, orange; motif B, blue; motif C, red; motif D, purple; and motif E, green. Val³⁹¹, identified as important for the binding of viral protein 3AB (14), is shown in yellow. The metal ion at the active site is shown in aqua.

conserved among RNA-dependent RNA polymerases; the positions of Val³⁹¹ and several motifs conserved among polymerases are shown in Fig. 1 (26). According to the frequently used analogy comparing polymerase structures to right hands, the “thumb” of polymerases such as HIV¹ reverse transcriptase, *Taq* DNA polymerase, and T7 DNA polymerase binds to the double-stranded portion of the template strand, positioning the primer, the 3'-hydroxyl of the nascent strand, at the active site (reviewed in Ref. 27). The precise orientations of the template, the protein primer, and the nascent RNA strand in the poliovirus polymerase structure are not yet known.

To define the 3AB binding site further and to determine whether residues in that site are important for 3B uridylylation, mutagenesis of the surface residues that surround the V391L mutation was undertaken. The ability of 14 mutant polymerases to bind to viral protein 3AB, catalyze RNA-dependent RNA polymerization, and uridylylate 3B was determined. The wild-type identities of several clustered surface residues near motif E were found to be involved in all 3AB- and 3B-mediated functions. Flanking residues appear to have additional functions in the enzymology of protein priming.

EXPERIMENTAL PROCEDURES

Plasmids and Mutagenesis—Mutations were introduced into the pT5T3D plasmid, designed to express polymerase 3D in *E. coli*, using the QuikChange mutagenesis protocol (Stratagene, La Jolla, CA) or the megaprimer method (28) with the primers described in Table I. The flanking primers for the megaprimer mutagenesis were CTGGGAG-CAATAAAG and CCCAGGAGTGATAACAGGTTTCAGCAGTGGG, amplifying the coding region of 3D polymerase from nucleotide 606–1348. The PCR products were cleaved with *Nsi*I and *Mfe*I (New England Biolabs, Beverly, MA) and inserted into similarly cleaved wild-type pT5T3D. The mutations were confirmed by sequencing.

To construct two-hybrid bait plasmids, the 3D polymerase coding region was amplified from mutant pT5T3D using primers CCGAATTCGGTGAAATCCAGTGGATGAGA and CGGGATCCTCGAGTTACTAAATGAGTCAAGCC, cleaved with *Eco*RI and *Bam*HI, and cloned into pLex202+PL (29). The appropriate sequence in all plasmids constructed using PCR was confirmed by sequencing.

3D Polymerase Purification and Activity Assays—Wild-type and mutant poliovirus polymerases were purified as described previously (30). Activity assays were performed with 2 μ M polymerase in 50 mM HEPES (pH 7.5), 0.5 mM MnCl₂, 50 μ M ZnSO₄, 30 mM NaCl, 70 μ g/ml poly(A) (200 μ M nucleotide), 25 μ g/ml oligod(T)₁₆ (100 μ M nucleotide), 400 μ M UTP, and 1 μ Ci/ml [α -³²P]UTP (3000 Ci/mmol; PerkinElmer Life Sciences). Reactions were incubated for 10 min on ice, incubated for 30 min at 30 °C, and spotted onto DE81 paper wetted in wash (5% dibasic sodium phosphate and 2% sodium pyrophosphate (w/v)). The paper was washed five times for 5 min in 200 ml of wash and then washed for 1 min in 200 ml of distilled H₂O and 1 min in 200 ml of 95% ethanol. The paper was allowed to dry, and bound ³²P was quantified using a PhosphorImager (Molecular Dynamics).

Two-hybrid Analysis—For expression in the yeast two-hybrid system, the coding regions of wild-type polymerase and all mutant polymerases that were successfully expressed in *E. coli* were cloned into the C-terminal coding region of a *lexA*-encoding “bait” plasmid (29). Expression of these *lexA*-polymerase bait proteins was comparable to that of the wild-type *lexA*-polymerase fusion protein (data not shown; Ref. 14). β -Galactosidase assays were performed as described previously (14) by the permeabilized cell method of Miller (31). Cells were grown at 30 °C in medium containing 2% raffinose to A₆₀₀ = 0.1/cm. Galactose was then added to 2% (w/v), and cells were incubated at 25 °C until they reached A₆₀₀ = 0.3/cm, at which time the cells were harvested.

Preparation of 3AB-containing *E. coli* Membranes—Membranes containing 3AB were prepared basically according to the protocol of Lama *et al.* (20). *E. coli* (BL21) containing pKK3AB (20) were grown in LB with 150 μ g/ml ampicillin at 37 °C to A₆₀₀ = 0.5/cm. The cultures were then grown at 22 °C until they reached A₆₀₀ = 0.75/cm, at which time they were induced with 0.5 μ M isopropyl-1-thio- β -D-galactopyranoside. The cultures were harvested by centrifugation at 11,000 \times g at 4 °C (8500 rpm in a Beckman JA-14 rotor) for 5 min. The cells were resuspended in 25 ml of ice-cold 100 mM NaCl, 50 mM Tris-HCl (pH 7.6), and 5% glycerol and harvested as described above. This wash step was repeated one additional time. The final pellet was frozen at -80 °C. The pellet was thawed and resuspended on ice in 10 ml/liter original culture of Buffer A (100 mM NaCl, 50 mM Tris-HCl (pH 7.6), 5% glycerol, 1 mM phenylmethylsulfonyl fluoride, 1 mM EDTA, 1 mM dithiothreitol, and 1 \times Complete Protease Inhibitor Mixture (Roche Molecular Biochemicals)). This suspension was lysed by passage through a chilled French press at 16,000 p.s.i. The lysate was cleared by centrifugation at 10,000 \times g for 40 min in a Beckman JA-20 rotor at 9000 rpm at 4 °C. The membrane fraction was collected by centrifugation at 24,000 rpm for 30 min (100,000 \times g) in a Beckman SW-41Ti rotor at 4 °C. The pellet was resuspended to 12.5 mg/ml protein in Buffer A and stored at -80 °C. Control membranes were prepared identically from cells harboring the pGEM vector.

Polymerase Recruitment Assay—Ten μ l of membranes (125 μ g of total protein) was mixed with 30 μ l of a preparation that contained 5 μ M wild-type or mutant polymerase, diluted using the buffers from the final column of the purification (100 mM NaCl, 25 mM Tris-HCl (pH 8.5), 15% glycerol, 0.5% octyl- β -glucopyranoside, 0.1 mM EDTA, 0.02% NaN₃, 2 mM dithiothreitol) and glycerol to 40% and 600 mM NaCl. The reaction was incubated on ice for 1 h and then incubated at 30 °C for 20 min. The reaction was spun at 14,000 rpm (16,000 \times g) at room temperature for 5 min. The supernatant was removed, and the pellet was resuspended in 100 μ l of wash buffer (500 mM NaCl, 25 mM Tris-HCl (pH 8.0), and 10 mM dithiothreitol). The membranes were collected by centrifugation as described above, and the pellet was resuspended in 8 μ l of 2 \times SDS-PAGE buffer (32), vortexed, and boiled for 4 min. The proteins were

¹ The abbreviation used is: HIV, human immunodeficiency virus.

TABLE I
Introduced mutations in 3D polymerase, mutagenic oligonucleotides, and sources of plasmids

Mutation	Oligonucleotide ^a /source of plasmid	Purified?	Comments
Y326A	CTAAAAATGATTGCCGCGGGTGATGATG ^b	Yes	
D328A/D329A	Diamond <i>et al.</i> (Ref. 50)	Yes	
D358A	GACTCCAGCTGCCAAATCAGCTAC ^b	Yes	
K359A	GACTCCAGCTGACGCGTCAGCTACATTTG ^c	Yes	
E369A	GTCACATGGGCCAATGTAACATTC ^b	Yes	
N370A	GTCACATGGGAGGCTGTAACATTC ^b	No ^d	
K375A	GTAACATTCTTGCGGAGATTCTTCAGG ^c	Yes	
R376A	GTAACATTCTTGAAGGCATTCTTCAGGG ^c	No ^d	
F377A	CATTCTTGAAGAGAGCCTTCAGGGCAGACG ^c	Yes	
R379A	GAGATTCTTCGCGGCAGACGAGAAATAC ^c	Yes	Decreased solubility
R379E	GAAGAGATTCTTCGAGGCAGACGAGAAATACCC ^b	Yes	
E382A	CTTCAGGGCAGACGCGAAATACCC ^b	Yes	
H389A	CCCATTCTTATCGCGCCAGTAATGCC ^c	No ^d	
V391L	Hope <i>et al.</i> (Ref. 14)	Yes	ts in virus
P393A	ATCCAGTAATGGCGATGAAGGAAAT	No ^d	
M394T	Barton <i>et al.</i> (Ref. 35)	Yes	ts in virus
K395A	CCAGTAATGCCAATGGCGGAAATTCATG ^c	Yes	
N424D	Burns <i>et al.</i> (Ref. 34)	No ^d	ts in virus
N424H	Burns <i>et al.</i> (Ref. 34)	Yes	ts in virus
N424Y	Burns <i>et al.</i> (Ref. 34)	No ^d	ts in virus

^a Introduced mutations are underlined. Oligonucleotides were purchased from Stanford Protein and Nucleic Acids Facilities or OPERON Technologies.

^b Mutation introduced into pT5T3D using megaprimer PCR mutagenesis (28).

^c Mutation introduced into pT5T3D with the oligonucleotide shown and the complementary oligonucleotide using the QuikChange site-directed mutagenesis kit (Stratagene).

^d Polymerase does not purify well, may be malformed or poorly expressed.

resolved on a 12.5% SDS gel (29:1, acrylamide:bis). The gel was stained with Sypro Red (Molecular Dynamics) diluted 1:5000 in 7.5% acetic acid for 30 min at room temperature with gentle rocking. The gel was destained for 30 min in 7.5% acetic acid. Staining was visualized using the Molecular Dynamics Storm in red fluorescence mode. Quantitation was performed with ImageQuant software (Molecular Dynamics).

3B Uridylation—Wild-type and mutant polymerase preparations were adjusted to 20 μ M polymerase, 50% glycerol, and 150 mM NaCl using the buffers from the final column of the purification and glycerol. 30 μ l of solution that contained 10 μ l of 75% acetonitrile and 20 μ l of column buffer supplemented to 4 M NaCl was added to 100 μ l of polymerase. The mixture was incubated on ice for 1 h. An aliquot (100 μ l) of the mixture was dialyzed against 100 mM NaCl and 50% glycerol for 6 h. (Slide-A-Lyzer Mini Dialysis Units; Pierce). Protein concentration was then adjusted to 10 μ M polymerase with dialysis buffer. Polymerase (10 μ l) was then added to 40 μ l of reaction buffer to final concentrations of 50 mM HEPES (pH 7.5), 2 mM dithiothreitol, 0.5 mM MnCl₂, 8% glycerol, 140 μ g/ml poly(A) (400 μ M/nt), 200 μ M 3B (VPg), 2 μ M UTP, and 10 μ Ci/ml [α -³²P]UTP (3000 Ci/mmol; PerkinElmer Life Sciences), and the reactions were incubated at 30 °C for 30 min. The reaction was stopped by the addition of 100 μ l of 2 \times SDS-PAGE buffer. The products were resolved on a 12% (29:1, acrylamide:bis) Tris-tricine gel. The gel was dried onto 3MM Whatman paper and analyzed by PhosphorImager (Molecular Dynamics). Quantitation was performed with ImageQuant (Molecular Dynamics).

Structure Analysis—Analysis of the crystal structure of poliovirus 3D polymerase was performed using Swiss-PDB Viewer (Ref. 33; available at www.expasy.ch/spdbv/) using coordinates from Hansen *et al.* (26). Images were rendered using POV-Ray freeware (available at www.povray.org).

RESULTS

Mutagenesis of a Candidate Surface for 3AB Binding on the Poliovirus Polymerase—We predicted that if the genetic screen that identified the V391L mutation accurately identified the 3AB binding site on the poliovirus polymerase (14), then polymerases that contained mutations in residues adjacent to Val³⁹¹ should display phenotypes similar to that of the V391L polymerase. Mutations were introduced into 14 additional residues surrounding Val³⁹¹, as shown on the three-dimensional structure of polymerase (26) in Fig. 5A and summarized in Table I. For Asp³⁵⁸, Lys³⁵⁹, Glu³⁶⁹, Glu³⁷⁰, Lys³⁷⁵, Arg³⁷⁶, Phe³⁷⁷, Arg³⁷⁹, Glu³⁸², His³⁸⁹, Pro³⁹³, and Lys³⁹⁵, codons that encode alanine were substituted for the wild-type codons (Table I). Mutational analyses of Asn⁴²⁴ (changed to Asp, His, and

Tyr) and Met³⁹⁴ (changed to Thr) have been described previously, and the resulting viruses have been shown to be temperature-sensitive for RNA synthesis (34, 35). Therefore, the published mutations N424D, N424H, N424Y, and M394T were introduced at these positions. Because the R379A mutant polymerase exhibited decreased solubility, making it unsuitable for direct binding assays, an additional mutant polymerase, R379E, was created. Mutant polymerases D358A, K359A, E369A, K375A, F377A, R379A, R379E, E382A, V391L, M394T, K395A, and N424H were successfully expressed and purified.

Mutations in Three Clustered Residues in the Poliovirus Polymerase Cause Specific Defects in Binding to Viral Protein 3AB in the Two-hybrid System—The effects of mutations in the putative 3AB-binding domain of poliovirus polymerase on its interactions with 3AB in the two-hybrid system are shown in Fig. 2. Testing the effect of these mutations on the interaction of polymerase with known ligands in addition to 3AB provided controls for proper folding of the lexA-polymerase bait fusion protein. Those mutations that conferred a defect in polymerase binding to the 3AB “prey” but not to other preys (human Sam68 protein or other polymerase molecules) were considered to confer specific defects in 3AB binding (13, 14, 36).

Mutations F377A, R379A, R379E, and V391L all caused specific defects in polymerase-3AB binding (Fig. 2, *first two rows*). However, mutations in flanking residues D358A, K359A, E369A, E370A, K375A, E382A, M394T, K395A, and N424Y had no significant effect on the interaction of polymerase with 3AB, other polymerase molecules, or Sam68 (Fig. 2). Therefore, Phe³⁷⁷, Arg³⁷⁹, and Val³⁹¹ are likely to constitute at least part of the 3AB binding site, as summarized in Fig. 5B.

Effect of Polymerase Mutations on Binding to Membrane-associated 3AB—To test the effect of mutations on the ability of the polymerase to bind 3AB outside of the context of a fusion protein, membranes that contained 3AB were used to recruit mutant and wild-type 3D polymerases from solution. *E. coli* membranes were prepared from cells that did or did not express plasmid-encoded 3AB. Equivalent amounts of these membranes were used as affinity matrices to recruit soluble polymerases from solution. Whereas expression of 3AB in eukaryotic systems has been reported (19, 25), these expression

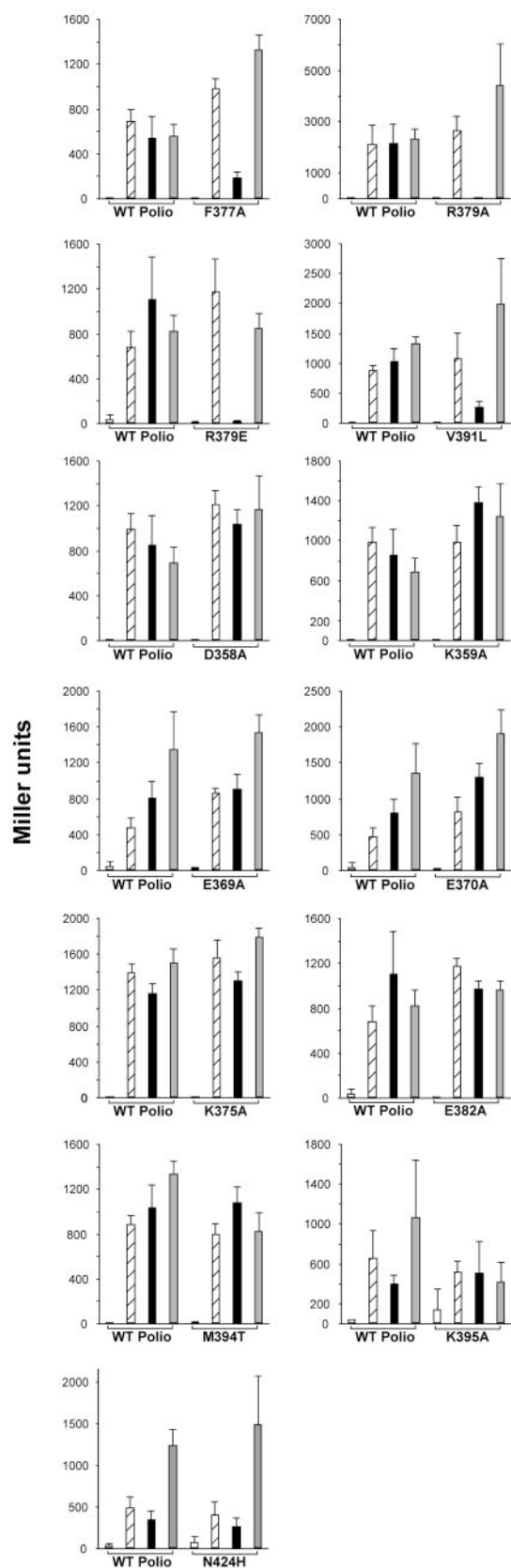


FIG. 2. Two-hybrid analysis of the interaction of mutant poliovirus polymerases with 3AB and two other ligands. Wild-type and mutant poliovirus polymerase sequences were expressed as bait *lexA* fusion proteins (29) in *Saccharomyces cerevisiae* to similar cellular concentrations and did not affect the expression or accumulation of prey proteins (data not shown). The amounts of β -galactosidase activity are therefore an indication of the relative affinities of the wild-type and

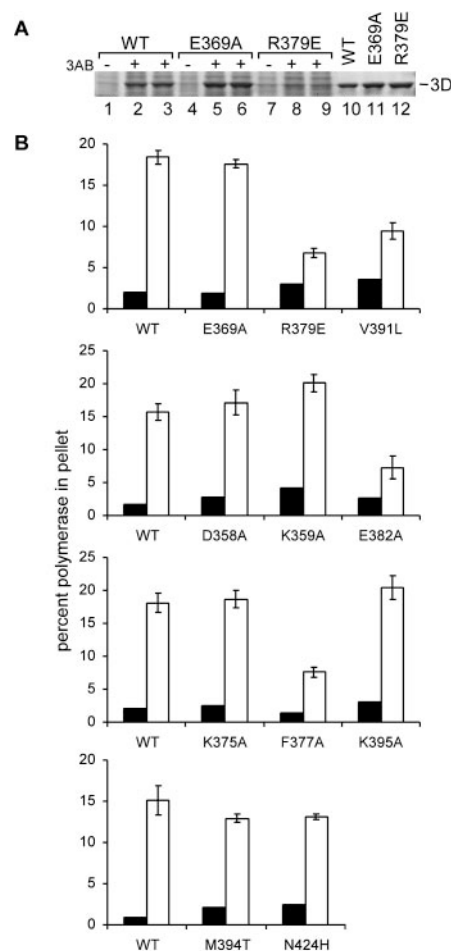


FIG. 3. Ability of membrane-bound 3AB to recruit wild-type and mutant poliovirus polymerases from solution. Membranes were prepared from *E. coli* that did not express (-) and did express (+) poliovirus 3AB protein ("Experimental Procedures"). After incubation of membrane preparations (175 μ g of total protein) with solutions containing 5 μ M wild-type (WT) or mutant polymerases, the percentage of polymerase that precipitated with the membranes was determined by comparison of the amount of precipitated polymerase to total polymerase on a SyproRed-stained gel (Molecular Dynamics) as shown in A. The results shown in A for E369A and R379E polymerases, as well as the results for nine other mutant polymerases, are quantified in B. Polymerase recruitment by *E. coli* membranes that did not contain 3AB is indicated by ■, and polymerase recruitment by *E. coli* membranes that contained 3AB is shown by □. S.D. values from duplicate experiments performed for polymerase binding to 3AB-containing membranes are indicated. The results of these experiments are summarized in Fig. 5C.

levels are low (37), so that obtaining sufficient quantities from these systems to perform the analyses reported here would be difficult.

As shown in Fig. 3A, the presence of 3AB in the membranes allowed the recruitment from solution of wild-type polymerase (lanes 2 and 3) and E369A mutant polymerase (lanes 5 and 6). However, recruitment was significantly disturbed by the R379E mutation (lanes 8 and 9), even though equivalent amounts of all polymerases were present in the reaction mix-

mutant polymerase baits for each of the three different prey proteins, expressed as fusions with a transcriptional activation domain (29). For each experiment, both the interactions displayed by the mutant polymerase bait and the interactions displayed by a wild-type control performed in the same experiment are shown. □, control prey vector; ▨, wild-type poliovirus polymerase; ■, 3AB prey; ▤, human Sam68 protein. For each graphed value of β -galactosidase activity, the average value (expressed in Miller units) and the S.E. observed from three to five different cultures are indicated. These data are summarized in Fig. 5B.

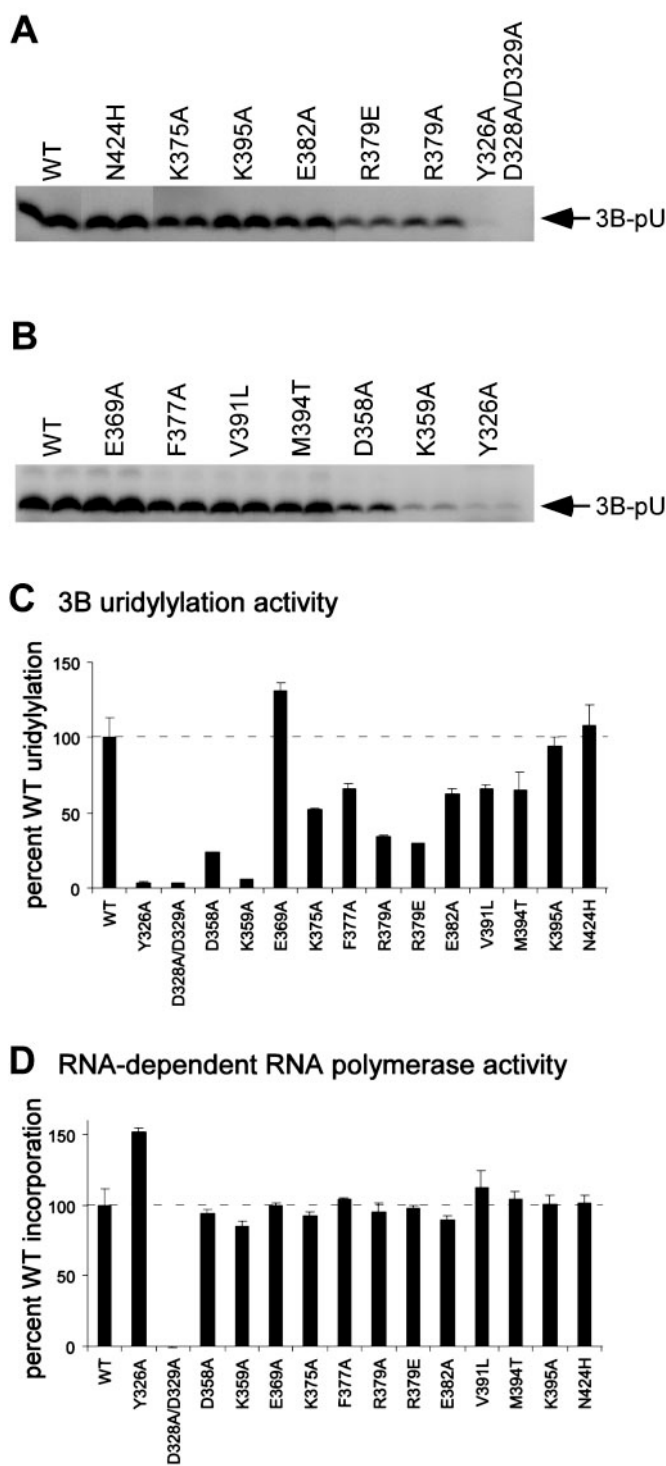


FIG. 4. Effect of mutations in the 3AB binding site on 3D polymerase on the uridylylation of 3B and on RNA-dependent RNA polymerase activity. Assays to measure the uridylylation of 3B (200 μM) by wild-type and mutant polymerases (2 μM) were performed as described (see “Experimental Procedures”). The 30 min time point chosen reflects the initial rate of the reaction under these conditions, and the amount of incorporated ^{32}P from [$\alpha\text{-}^{32}\text{P}$]UTP was linearly responsive to the concentration of 3B for wild-type and mutant polymerases (data not shown). ^{32}P -labeled proteins were displayed by SDS-PAGE on a 12% Tris-tricine gel and imaged with a PhosphorImager (Molecular Dynamics). Two sets of experiments are shown in A and B. With the exception of the D328A/D329A polymerase, experiments were performed in duplicate. The results are quantified in C, and the S.D. is shown. RNA-dependent RNA polymerase activity was determined for the wild-type and mutant polymerases in a poly(A)/oligo(dT)₁₆ assay at 2 μM polymerase as described under “Experimental Procedures” (D). These results are summarized in Fig. 5D.

tures (lanes 10–12). These data and similar data for other mutant polymerases are quantified in Fig. 3B, where the amounts of wild-type and mutant polymerases recruited by the 3AB-containing membranes are compared for several independent experiments. Consistent with the results of the two-hybrid experiments, mutant polymerases R379E, V391L, and F377A all displayed reduced binding to the 3AB-containing membranes. In addition, E382A mutant polymerase displayed reduced binding, whereas none of the other mutant polymerases displayed significantly reduced interactions with membrane-associated 3AB. These data are summarized on the three-dimensional structure of the polymerase in Fig. 5C. The clustering of the residues in a hydrophobic pocket on the protein surface and the lack of apparent misfolding of the mutant polymerases argue that these residues identify a site of direct 3AB binding.

Mutations in the 3AB Binding Site and Several Flanking Residues Decrease 3B Uridylylation—It is not clear whether the 3AB binding site on poliovirus polymerase identified the binding site for 3B as well. However, available evidence (see “Introduction”) supports the hypothesis that important contacts for 3AB with polymerase are contained in the 3B sequences. In addition, the 3AB binding site identified by two-hybrid and membrane recruitment assays (Fig. 5, B and C) is close to the active site for phosphodiester bond formation (26), making the 3AB binding site an attractive candidate for the binding of the 3B sequences during uridylylation.

To determine whether mutations in the binding sites for 3AB affect 3B uridylylation, 12 different mutant polymerases whose effects on the binding of 3AB had been defined (Figs. 2 and 3) and 2 mutant polymerases that contained mutations in the active site for polymerization (Y326A and D328A/D329A) were studied. Uridylylation of 3B was quantified during the initial, linear phase of the uridylylation reaction (data not shown), therefore giving a measure of the reaction rate. As can be seen from the direct labeling of 3B by $\alpha\text{-}^{32}\text{P}$ UTP (Fig. 4, A and B), several of the mutant polymerases showed decreased rates of 3B uridylylation relative to wild-type polymerase, although two (N424H and K395A) showed no apparent change, and one (E369A) showed an apparent stimulation of this rate. These data are summarized in Fig. 4C. The residues for which mutations caused reductions in the rate of 3B uridylylation are shown on the three-dimensional structure in Fig. 5D.

The RNA-dependent RNA polymerase activity of each of these enzymes was tested under the conditions of saturating RNA concentrations present in the 3B uridylylation assays. As shown in Fig. 4D, all the mutant enzymes except D328A/D329A, which contains two mutations in the polymerase active site, showed at least wild-type RNA-dependent RNA polymerase activities. Therefore, for the D328A/D329A mutant polymerase, the observed failure to uridylylate 3B could be explained by its failure to perform any phosphoryl transfer reaction.

All of the mutations that interfered with 3AB binding in two-hybrid assays or in 3AB-mediated membrane recruitment (F377A, R379E, E382A, and V391L) showed reduced rates of 3B uridylylation (Fig. 4C). This is consistent with the idea that the 3AB binding site (Fig. 5, B and C) and the binding site for the 3B substrate during uridylylation are similar or overlapping.

Mutations in residues adjacent to the 3AB binding site showed mixed effects on the rate of 3B uridylylation. N424H and K395A polymerases showed no defect in either polymerization (Fig. 4D) or 3B uridylylation (Fig. 4C) under these conditions, although the residues are directly adjacent to the 3AB binding site. M394T polymerase, previously demonstrated to

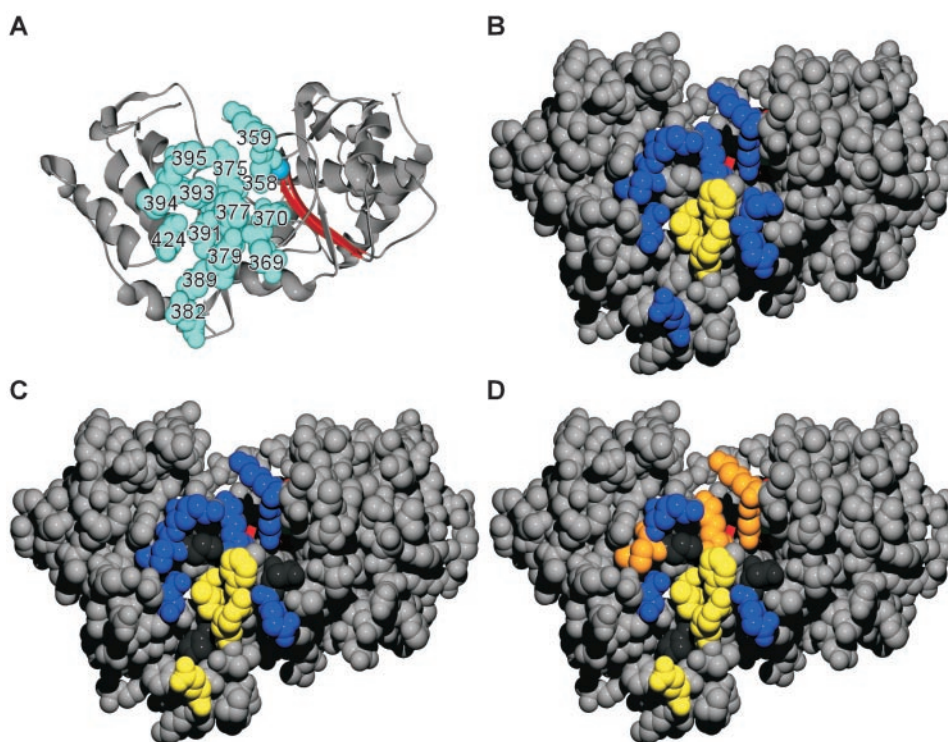


FIG. 5. Residues of 3D polymerase whose wild-type identity is important for 3AB binding and 3B uridylylation. The residues of the polymerase targeted for mutation are shown as *light blue space-filling representations* on a ribbon diagram of the polymerase viewed from the back (A). Motif C, which contains the YGDD sequences at the active site, is shown in *red*. The remaining panels summarize the results of the yeast two-hybrid (B), 3AB-mediated membrane recruitment (C), and 3B uridylylation assays (D). Residues that, when mutagenized, show a decrease in binding are shown in *yellow*, and those that have no effect are shown in *blue*. In D, those residues that were not found to be involved in binding of 3AB but that, when altered, reduce uridylylation of 3B are shown in *orange*. Other residues that, when altered, result in low expression of the polymerase in *E. coli* are shown in *black*. Arg³⁷⁶, when changed to Ala, reduced the expression of polymerase in *E. coli* and cannot be seen from this view.

be defective in both 3B uridylylation and RNA-dependent RNA polymerase activity (9), displayed a decreased rate of 3B uridylylation but not polymerase activity in these experiments (Fig. 4, C and D). It should be noted that in these experiments, initial rates of uridylylation and polymerization were measured, whereas previous studies measured the extents of these reactions. Therefore, the differences observed may be due to the lability of the M394T polymerase during extended incubation. Similar to our observations for M394T, defects in 3B uridylylation but not polymerase activity were demonstrated by D358A and K359A mutant polymerases.

Mutation of another residue near the active site of the polymerase, Y326A, caused an apparent stimulation in polymerase activity (Fig. 4D) but a dramatic reduction in the rate of 3B uridylylation (Fig. 4C). These results suggest that although the same active site is used for phosphoryl transfer with both nucleic acid and protein primers, the exact chemistry of the reactions may differ.

DISCUSSION

We have defined a binding surface for membrane-associated poliovirus protein 3AB on the three-dimensional structure of the viral RNA-dependent RNA polymerase 3D using yeast two-hybrid and direct binding assays. Mutations in residues Val³⁹¹, Phe³⁷⁷, and Arg³⁷⁹ interfered with 3AB binding in both assays (Fig. 5, B and C), whereas a mutation in residue Glu³⁸² showed a defect in the direct binding assay only (Fig. 5C), indicating that this assay is perhaps more sensitive than the two-hybrid assay. Although it is formally possible that these mutations interfere indirectly with 3AB binding, it is likely that they identify a region of direct contact between 3AB and the poly-

merase due to the lack of evidence of misfolding of the mutant polymerases and the physical clustering of the residues near a hydrophobic pocket on the polymerase surface (Fig. 5, B and C). Phe³⁷⁷, Arg³⁷⁹, Glu³⁸², and Val³⁹¹ are present at this position in 18.5%, 50.0%, 53.7%, and 74.1%, respectively, of picornavirus polymerases (38).

All the mutations that interfered with the binding of 3AB to polymerase (F377A, R379A, R379E, E382A, and V391L) also decreased the rate of 3B uridylylation by the polymerase (Figs. 4 and 5D) but had little effect on nucleic acid-primed polymerase activity under similar conditions (Fig. 4D), consistent with the hypotheses that the binding sites for 3B and 3AB overlap and that binding of 3B via these contacts is required for uridylylation. Similarly, several mutations in the DNA polymerase of Φ 29 phage that interfere with polymerase binding to terminal protein, the primer of DNA synthesis, abrogated terminal protein-primed DNA synthesis but not DNA synthesis primed with a DNA oligonucleotide (39). Therefore, the reduction in binding affinity for the protein primer is likely to provide one mechanism for reducing the rate of protein priming for both poliovirus and Φ 29 phage.

Mutations in some of the residues that surround the 3AB binding site, specifically, M394T, R358A, R359A, and K395A, also reduced the rate of 3B uridylylation (Figs. 4 and 5D) but showed little effect on either polymerase activity (Fig. 4D) or 3AB binding affinity (Fig. 5, B and C). Assuming that substrate binding is only one step in the uridylylation reaction, it is not surprising that the residues required for high-affinity binding of 3AB, and likely 3B as well, are only a subset of those required for catalysis. Similar mutations that decrease protein

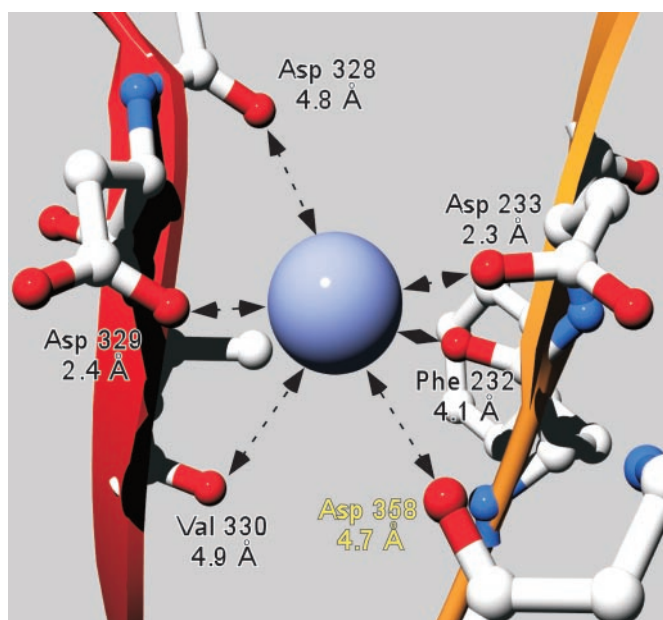


FIG. 6. Proximity of Asp³⁵⁸, required for 3B uridylylation but not 3AB binding, to the polymerase active site. Amino acid residues that contain atoms within 5 Å of the metal ion present at the active site of 3D polymerase (26) are shown. The Ca²⁺ ion present in the polymerase crystal is shown in *aqua*; this is presumably replaced by Mg²⁺ or Mn²⁺ during catalysis (26). The ribbon diagrams of the canonical polymerase domains are colored as described in Fig. 1 (motif A, orange; motif C, red).

primer utilization but not its binding have been characterized in the DNA polymerase of Φ 29 (Ref. 40 and the references therein).

The poliovirus RNA-dependent RNA polymerase catalyzes two different types of phosphoryl transfer reactions, the formation of internucleotide bonds during RNA elongation and the formation of tyrosine-phosphate bonds during the uridylylation of 3B (9). Both reactions involve pairing of the incorporated nucleotide with an RNA template. Mutations in the conserved YGDD sequences at the active site are known to alter metal specificity and to impair the ability of the enzyme to catalyze internucleotide bond formation (41, 42). As shown in Fig. 4, *C* and *D*, mutation of this YGDD sequence to YGAA destroyed the ability of polymerase 3D to form either internucleotide or tyrosine-phosphate bonds. However, mutation of Asp³⁵⁸, which contains atoms within 5 Å of the metal at the active site (Fig. 6), had no effect on the formation of internucleotide bonds but almost completely abrogated 3B uridylylation. Mutation of Lys³⁵⁹, a residue highly conserved in RNA-dependent polymerases, shares this phenotype. It is intriguing that, although widely conserved, Lys³⁵⁹ is not conserved in polymerases that perform *de novo* synthesis, such as those of hepatitis C and Φ 6. Similarly, mutation of Tyr³²⁶, the first conserved residue in the YGDD sequence, stimulated the formation of internucleotide bonds but destroyed the ability of polymerase 3D to perform 3B uridylylation (Fig. 4, *C* and *D*).

It is possible that differential effects of mutagenesis of the polymerase active site on tyrosine uridylylation and internucleotide bond formation result from different chemistries of these two reactions. For example, residues such as Tyr³²⁶ and Asp³⁵⁸ in the poliovirus polymerase may participate in metal chelation and phosphoryl transfer reactions during uridylylation of 3B, but not during internucleotide bond formation. In DNA topoisomerases, the same active site promotes four phosphoryl transfer reactions: the breakage of internucleotide phosphodiester bonds, the formation of a covalent bond between the active site tyrosine and the cleaved DNA, the cleavage of the tyrosine-DNA

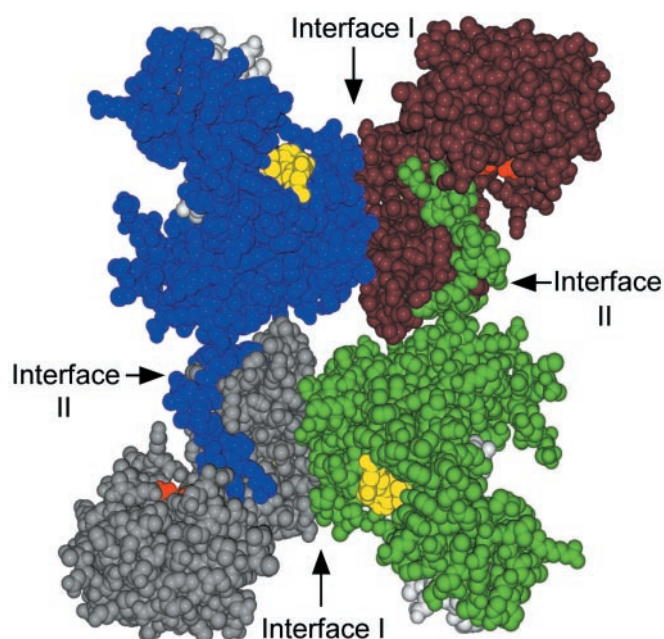


FIG. 7. Polymerase-polymerase interactions in the three-dimensional structure of poliovirus polymerase and location of the 3AB binding site. The unit cell of the crystal structure is shown, with each polymerase colored distinctly. Residues that constitute the 3AB binding site are shown in *yellow*. The GDD sequence at the active site is shown in *red*. Interface I can be seen as the abutment of polymerase monomers in the horizontal dimension. Interface II is apparent as the abutment of monomers in the vertical direction and the intermolecular donation of the N-terminal strand of one monomer into the thumb of the adjacent monomer. The N-terminal strands that are donated by monomers outside the unit cell are shown in *white*.

complex, and the formation of a new internucleotide bond. Several mutations in the active site can specifically reduce the rate of the later steps without affecting earlier steps (43–46).

Here we provide evidence that poliovirus protein 3AB can tether the soluble polymerase to membranes by direct binding via four residues on the polymerase surface, two of which are part of conserved motif E. Our data do not clarify whether the proteolytic liberation of 3B from 3AB or a larger precursor occurs before or after the protein priming reaction. However, the observation that membrane tethering by 3AB could place the protein primer 3B in the vicinity of the polymerase active site was shown by the inhibition of 3B uridylylation by mutation of the residues required for 3AB binding. This is the second time that a function for motif E in priming of RNA replication has been described: in the three-dimensional structure of Φ 6 RNA-dependent RNA polymerase, motif E appears to position the C-terminal domain, which in turn positions the GTP molecules used to initiate *de novo* RNA replication (47).

Poliovirus polymerase functions as an oligomer in solution (30, 48, 49). The three-dimensional structure of poliovirus polymerase revealed two intermolecular interfaces (26), as shown in Fig. 7. Disruption of either interface by mutagenesis correlates with loss of viral viability (30). Polymerase interactions via either Interface I or Interface II display head-to-tail orientations such that the polymerase oligomer could, in principle, continue indefinitely; the size of the oligomeric polymerase in infected cells has yet to be determined. As shown in Fig. 7, the 3AB binding site identified here does not overlap with any of the polymerase-polymerase interaction surfaces. Instead, membrane-associated 3AB could contact every second polymerase in a higher-order polymerase oligomer, consistent with the hypothesis that these protein-protein interactions occur in

the viral RNA replication complex to coordinate membrane association, protein priming, and RNA elongation.

Acknowledgments—We thank Ellie Ehrenfeld, Jeffrey L. Hansen and Scott D. Hobson for discussions of the polymerase structure and membrane association, Katya Smirnyagina for experimental contributions, and Aniko Paul for technical advice concerning the 3B uridylylation reaction. Comments on the manuscript from Peter Sarnow, Esther Bullitt, and Scott Crowder are gratefully acknowledged.

REFERENCES

- Baroudy, B. M., Venkatesan, S., and Moss, B. (1982) *Cell* **28**, 315–324
- deLange, A. M., Reddy, M., Scraba, D., Upton, C., and McFadden, G. (1986) *J. Virol.* **59**, 249–259
- Biessmann, H., Mason, J. M., Ferry, K., d'Hulst, M., Vlageirdottir, K., Traverse, K. L., and Pardue, M. L. (1990) *Cell* **61**, 663–673
- Salas, M. (1991) *Annu. Rev. Biochem.* **60**, 39–71
- Sun, X., Johnson, R., Hockman, M., and Wang, Q. (2000) *Biochem. Biophys. Res. Commun.* **268**, 798–803
- Zhong, W., Uss, A. S., Ferrari, E., Lau, J. Y., and Hong, Z. (2000) *J. Virol.* **74**, 2017–2022
- Luo, G., Hamatake, R. K., Mathis, D. M., Racela, J., Rigat, K. L., Lemm, J., and Colonno, R. J. (2000) *J. Virol.* **74**, 851–863
- Kim, M. J., Zhong, W., Hong, Z., and Kao, C. C. (2000) *J. Virol.* **74**, 10312–10322
- Paul, A. V., Boom, J. H., Filippov, D., and Wimmer, E. (1998) *Nature* **393**, 280–284
- Paul, A. V., Rieder, E., Kim, D. W., van Boom, J. H., and Wimmer, E. (2000) *J. Virol.* **74**, 10359–10370
- Rieder, E., Paul, A. V., Kim, D. W., van Boom, J. H., and Wimmer, E. (2000) *J. Virol.* **74**, 10371–10380
- Goodfellow, I., Chaudhry, Y., Richardson, A., Meredith, J., Almond, J. W., Barclay, W., and Evans, D. J. (2000) *J. Virol.* **74**, 4590–4600
- Xiang, W., Cuconati, A., Hope, D., Kirkegaard, K., and Wimmer, E. (1998) *J. Virol.* **72**, 6732–6741
- Hope, D. A., Diamond, S. E., and Kirkegaard, K. (1997) *J. Virol.* **71**, 9490–9498
- Chen, J., and Ahlquist, P. A. (2000) *J. Virol.* **74**, 4310–4318
- Suhy, D. A., Giddings, T. H. J., and Kirkegaard, K. (2000) *J. Virol.* **74**, 8158–8165
- Teterina, N. L., Egger, D., Bienz, K., Brown, D. M., Semler, B. L., and Ehrenfeld, E. (2001) *J. Virol.* **75**, 3841–3850
- Towner, J. S., Ho, T. V., and Semler, B. L. (1996) *J. Biol. Chem.* **271**, 26810–26818
- Datta, U., and Dasgupta, A. (1994) *J. Virol.* **68**, 4468–4477
- Lama, J., Paul, A. V., Harris, K. S., and Wimmer, E. (1994) *J. Biol. Chem.* **269**, 66–70
- Paul, A. V., Cao, X., Harris, K. S., Lama, J., and Wimmer, E. (1994) *J. Biol. Chem.* **269**, 29173–29181
- Plotch, S. J., and Palant, O. (1995) *J. Virol.* **69**, 7169–7179
- Richards, O. C., and Ehrenfeld, E. (1998) *J. Biol. Chem.* **273**, 12832–12840
- Rodriguez-Wells, V., Plotch, S. J., and DeStefano, J. J. (2001) *Nucleic Acids Res.* **29**, 2715–2724
- Towner, J. S., Mazanet, M. M., and Semler, B. L. (1998) *J. Virol.* **72**, 7191–7200
- Hansen, J. L., Long, A. M., and Schultz, S. C. (1997) *Structure* **5**, 1109–1122
- Jager, J., and Pata, J. D. (1999) *Curr. Opin. Struct. Biol.* **9**, 21–28
- Ke, S. H., and Madison, E. L. (1997) *Nucleic Acids Res.* **25**, 3371–3372
- Gyuris, J., Golemis, E., Chertkov, H., and Brent, R. (1993) *Cell* **75**, 791–803
- Hobson, S. D., Rosenblum, E. S., Richards, O. C., Richmond, K., Kirkegaard, K., and Schultz, S. C. (2001) *EMBO J.* **20**, 1153–1163
- Miller, J. H. (1972) *Experiments in Molecular Genetics*, Cold Spring Harbor Laboratory, Cold Spring Harbor, NY
- Laemmli, U. K. (1970) *Nature* **227**, 680–685
- Guex, N., and Peitsch, M. S. (1997) *Electrophoresis* **18**, 2714–2723
- Burns, C. C., Richards, O. C., and Ehrenfeld, E. (1992) *J. Virol.* **189**, 568–582
- Barton, D. J., Morasco, B. J., Eisner-Smerage, L., Collis, P. S., Diamond, S. E., and Hewlett, M. J. (1996) *Virology* **217**, 459–469
- McBride, A. E., Schlegel, A., and Kirkegaard, K. (1995) *Proc. Natl. Acad. Sci. U. S. A.* **93**, 2296–2301
- Barco, A., and Carrasco, L. (1995) *Gene (Amst.)* **156**, 19–25
- Hobson, S. D. (2000) *Crystallographic and Biochemical Studies of Higher Order Poliovirus Polymerase Structures*. Ph.D. thesis, University of Colorado
- Dufour, E., Mendez, J., Lazazro, J. M., De Vega, M., Blanco, L., and Salas, M. (2000) *J. Mol. Biol.* **304**, 289–300
- Meijer, W. J., Horcajadas, J. A., and M. Salas. (2001) *Microbiol. Mol. Biol. Rev.* **65**, 261–287
- Jablonski, S. A., Luo, M., and Morrow, C. D. (1991) *J. Virol.* **65**, 4565–4572
- Jablonski, S. A., and Morrow, C. D. (1993) *J. Virol.* **67**, 373–381
- Chen, S.-J., and Wang, J. C. (1998) *J. Biol. Chem.* **273**, 6050–6056
- Zhu, C.-X., Roche, C. J., Papanicolaou, N., Dipietrantonio, A., and Tse-Dinh, Y.-C. (1998) *J. Biol. Chem.* **273**, 8783–8789
- Wittschieben, J., Peterson, B. O., and Shuman, S. (1999) *Nucleic Acids Res.* **26**, 490–496
- Fertala, J., Vance, J. R., Pourquier, P., Pommier, Y., and Bjornsti, M.-A. (2000) *J. Biol. Chem.* **275**, 15346–15253
- Butcher, S. J., Grimes, J. M., Makeyev, E. V., Bamford, D. H., and Stuart, D. I. (2001) *Nature* **410**, 235–240
- Pata, J. D., Schultz, S. C., and Kirkegaard, K. (1995) *RNA (N. Y.)* **1**, 466–477
- Beckman, M. T., and Kirkegaard, K. (1998) *J. Biol. Chem.* **273**, 6724–6730
- Diamond, S. E., and Kirkegaard, K. (1994) *J. Virol.* **68**, 863–876